Available online at www.sciencedirect.com
ScienceDirect
Journal of Sound and Vibration 315 (2008) 176–196
JOURNAL OF SOUND AND VIBRATION
www.elsevier.com/locate/jsvi

# Nonconservative stability problems via generalized differential quadrature method

Alessandro Marzani, Francesco Tornabene, Erasmo Viola*

*DISTART, Department of Structural Engineering, University of Bologna, Viale Risorgimento 2, Bologna I-40136, Italy*

Received 8 June 2007; received in revised form 10 December 2007; accepted 23 January 2008
Handling Editor: A.V. Metrikine
Available online 12 March 2008

**Abstract**

In this paper, the generalized differential quadrature (GDQ) method is applied to solve classical and nonclassical nonconservative stability problems. Various cantilever beams subjected to slope-dependent forces are considered. First, the governing differential equation for a nonuniform column subjected to an arbitrary distribution of compressive subtangential follower forces is obtained. The effect of the variability of the mechanical properties along the beam length is also considered. Then, the application of the GDQ procedure leads to a discrete system of algebraic equations from which the system critical loads can be obtained by solving an associated eigenvalue problem. A parametrical study for different levels of nonconservativeness of the applied load is carried out for some classical benchmark cases such as Beck's, Leipholz's and Hauger's column problems. Finally, applications to geometrically and mechanically tapered beams subjected to nonpotential subtangential follower forces are investigated as nonclassical cases.

It has been proved that the method can efficiently solve structural nonconservative elastic problems and, more in general, problems governed by a nonsymmetric system of algebraic equations.


## 1. Introduction

According to the critical overview given by Elishakoff [1], and in some of the papers herein quoted, the elastic stability problem for a cantilever column subjected to a compressive concentrated follower force at the tip end was firstly investigated by Reut in 1939. By applying the Euler static criterion of stability, Reut could not find any critical load for the system. Nikolai, observing the work of Reut, recognized the deficiency of the static criterion and the need of using a dynamic approach to study the stability of such nonconservative problem. He demonstrated his hypothesis finding with a dynamic criterion the critical load for a different problem that, in accordance with Reut, had only stable solution. Independently of the studies of Reut and Nikolai, Pflüger in 1950, investigating the stability of a column under the action of a statically tip follower force, came to the paradoxical conclusion that a column was stable for any bounded follower force. Few years

*Corresponding author. Tel.: +39 051 209 3510; fax: +39 051 209 3495.
*E-mail addresses:* alessandro.marzani@mail.ing.unibo.it (A. Marzani), francesco.tornabene@mail.ing.unibo.it (F. Tornabene), erasmo.viola@mail.ing.unibo.it (E. Viola).

0022-460X/$ - see front matter © 2008 Elsevier Ltd. All rights reserved.
doi:10.1016/j.jsv.2008.01.056

**Nomenclature**

| | |
|---|---|
| $A$ | beam cross-section area |
| $E$ | modulus of elasticity |
| $I$ | beam second area moment of inertia |
| $\mathbf{K}_b$ | total stiffness matrix of the boundary points with dimension $4 \times \mathcal{N}$ |
| $\mathbf{K}_d$ | total stiffness matrix of the domain points with dimension $(\mathcal{N}-4) \times \mathcal{N}$ |
| $\mathbf{K}^e$ | elastic stiffness matrix of the domain points with dimension $(\mathcal{N}-4) \times \mathcal{N}$ |
| $\mathbf{K}^g$ | geometric stiffness matrix of the domain points with dimension $(\mathcal{N}-4) \times \mathcal{N}$ |
| $\mathbf{K}^{nc}$ | nonconservative stiffness matrix of the domain points with dimension $(\mathcal{N}-4) \times \mathcal{N}$ |
| $L$ | beam length |
| $\mathsf{L}^{(1)}$ | Lagrange interpolating polynomial (first derivative) |
| $\mathbf{M}_d$ | diagonal mass matrix of the domain points with dimension $(\mathcal{N}-4) \times (\mathcal{N}-4)$ |
| $N$ | internal axial load |
| $\mathcal{N}$ | total number of the sampling points |
| $P$ | modulus of the subtangential concentrated compressive force |
| $q$ | law of distribution of the subtangential distributed force |
| $q_0$ | modulus of the subtangential distributed force at $x=0$ |
| $q_\alpha$ | distribution of the subtangential force |
| $Q_B$ | dimensionless load parameter for Beck's problem |
| $Q_{BT}$ | dimensionless load parameter for the geometrical tapered beam |
| $Q_{BM}$ | dimensionless load parameter for the mechanical tapered beam |
| $Q_H$ | dimensionless load parameter for Haugher's problem |
| $Q_L$ | dimensionless load parameter for Leipholz's problem |
| $Q_Q$ | dimensionless load parameter for the case with quadratic law distribution of subtangential load |
| $r$ | cross-section radius of the circular beam |
| $t$ | time |
| $T$ | system kinetic energy |
| $v$ | beam deflection |
| $V$ | beam transverse displacement |
| $W_c$ | conservative work |
| $\delta W_{nc}$ | nonconservative virtual work |
| $x$ | beam axis |
| $\alpha$ | nonconservativeness parameter |
| $\beta_{ij}^{(n)}$ | $n$th-order weighting coefficient at the $i$th point calculated for the $j$th point |
| $\gamma$ | mechanical tapered parameter |
| $\boldsymbol{\delta}$ | vector of displacements at the grid points with dimension $\mathcal{N} \times 1$ |
| $\boldsymbol{\delta}_b$ | vector of displacements at the boundary points with dimension $4 \times 1$ |
| $\boldsymbol{\delta}_d$ | vector of displacements at the domain points with dimension $(\mathcal{N}-4) \times 1$ |
| $\eta$ | geometrical tapered parameter |
| $\mu$ | material density |
| $\varphi$ | beam cross-section rotation |
| $\Phi$ | system elastic energy |
| $\omega$ | system eigenfrequency |
| $\Omega$ | dimensionless eigenfrequency parameter |

later, Ziegler, by applying the dynamic approach to a perfect two-degrees-of-freedom system subjected to the action of a concentrated compressive follower force, showed that the system would lose its stability dynamically. Finally, Beck [2], under the guidance of Ziegler, proved in 1952 that Euler's column tangentially loaded was susceptible to instability. It was thus recognized that elastic systems could lose stability not only via an instantaneous and irreversible change of configuration (divergence) but also via an exponential increasing motion with time (flutter).

This pioneering work established the inadequacy of the static approach to characterize the stability of some nonconservative systems, for which the dynamic approach was exclusive. Over the next 20 years approximately, the revolutionary outcome was investigated in depth and confirmed by numerous scientists such as Bolotin [3], Timoshenko and Gere [4], Nemat-Nasser [5] and Leipholz [6].

Afterwards, some investigations on the stability of an elastic column subjected to both follower (nonconservative) and axial (conservative) compressive forces were carried out aimed at clarifying the difference between conservative and nonconservative problems. For example, McGill [7] studied the effect of column weight on the flutter load of a cantilever beam subjected to uniform distribution of follower forces. Sundasarajan [8] introduced a nonconservativeness parameter, as the ratio between the

follower and axial component of tangential forces, to explore the change in stability regions between divergence and flutter. Such studies showed new results that were not observed before in studying purely nonconservative systems.

Since then, many works have contributed to the understanding of nonconservative stability problems. Stability of discrete and continuous systems such beams, plates and cylinders under the action of tangential and subtangential follower forces, has been largely studied. Critical comprehensive literature reviews on this subject are given by Elishakoff [1] and Langthjem and Sugiyama [9].

In the above papers it is shown that several analytical and numerical methodologies have been used to solve nonconservative stability problems; however, it also emerges that the generalized differential quadrature (GDQ) method has been scarcely applied for solving such stability problems. The essence of this numerical method is that partial or total derivatives of a smooth function are evaluated by a weighted sum of function values at discrete points. The weighting coefficients are not related to a special physical problem and only depend on the assumed interpolating basis functions and on the spatial distribution of the discrete points [10].

The GDQ method has been proved to be well suited for solving self-adjoint boundary value problem governed by linear differential equations. For example, two of the authors have extensively used this technique for solving static and dynamic problems on arch-like and shell structures [11–14].

The GDQ technique has been widely used also for solving self-adjoint stability problems. For instance Sherbourne and Pandy [15] investigated the buckling of composite beams and plates, Gutierrez et al. [16] characterized the buckling of circular thin plates, Mirfakhraei and Redekop [17] studied via GDQ the stability of circular cylindrical shells. However, to the author's best knowledge only De Rosa and Auciello [18] applied the GDQ method to characterize the stability of a nonself-adjoint problem, namely a foundation beam compressed by concentrated subtangential forces acting at the beam's ends.

In this paper, the GDQ technique is applied to nonconservative stability beam problems by considering several different geometrical, mechanical and loading conditions.

Firstly, three well-known nonconservative stability problems named Beck's, Leipholz's and Hauger's column are investigated. Secondly, the stability of a uniform column loaded by a distribution of subtangential forces with magnitude that varies along the beam length with a quadratic law is studied. Finally, a parametrical study on the stability of geometrical and mechanical tapered beams under the action of subtangential forces are proposed as nonclassical cases.

A unified governing differential equations is obtained via the extended form of Hamilton's principle and then discretized via GDQ to an ordinary nonsymmetric algebraic system of equations. The study of the associated eigenvalue problem leads to a system divergence or flutter instability.

In order to verify the accuracy of the proposed formulation in solving nonself-adjoint stability problem, when possible, the results of this paper have been compared to literature references.

The main outcome of the paper is that the GDQ method can solve with high accuracy and efficiency structural nonconservative elastic problems and, more in general, problems governed by a nonsymmetric system of algebraic equations.

## 2. Governing differential equations

In this section, the unified differential governing equation and boundary conditions for an elastic cantilever Euler–Bernoulli beam of length $L$, with varying mechanical and geometrical properties along the beam length, loaded by conservative and nonconservative forces is obtained by means of Hamilton's variational principle.

Let us assume a Cartesian reference coordinate $x$–$y$–$z$ system such that the $x$-axis coincides with the geometrical axis of the nondeformed beam and the $y$- and $z$-axis are parallel to the principal axes of the cross-section of area $A = A(x)$. It is assumed that the beam deflects in the $x$–$y$ plane and $I = I(x)$ is the second area moment of inertia around the $z$-axis (see Fig. 1(a)). The material density $\mu = \mu(x)$ and the modulus of elasticity $E = E(x)$ can also vary along the beam length.

The deflection of the column is assumed to be small, so that, if $v = v(x, t)$ is the beam displacement at a point of abscissa $x$ and time $t$ along the $y$-axis, the angle $\varphi = \varphi(x, t)$ between the $x$-axis and the tangent to the elastic line of the beam can be approximated by $\varphi = \partial v/\partial x$, as represented in Fig. 1(b).

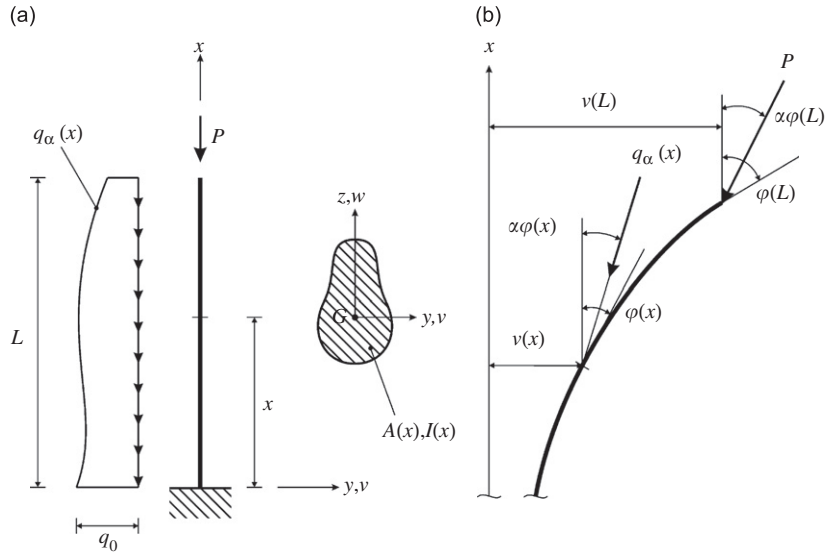


Fig. 1. (a) Cantilever beam subjected to a concentrated compressive subtangential force at the beam's end and to an arbitrary distribution of subtangential forces along the beam. (b) Schematic representation of the effect of the nonconservative parameter $\alpha$ on the loads applied to beam.

The column is subjected to a compressive subtangential concentrated force $P$, acting at $x = L$, and to a distribution of compressive subtangential force $q_\alpha(x) = q_0 q(x)$, where $q_0$ represents the magnitude of $q_\alpha$ at $x = 0$ and $q(x)$ is the distribution law of the subtangential force.

The grade of nonconservativeness of both subtangential force types, $P$ and $q_\alpha$, is defined by the nonconservativeness parameter $\alpha$, that sets the amount of tangential (follower) components of the forces for a variation of the beam configuration. In particular, as it can be seen in Fig. 1(b), $\alpha\varphi$ denotes the angle between the $x$-axis and the direction of the compressive subtangential force. For $\alpha = 0$ pure axial conservative forces are applied on the system, while pure tangential forces are accounted when $\alpha = 1$. Parametrical stability studies can thus be carried out by varying the parameter $\alpha$ from 0 to 1. In literature, $\alpha$ is usually referred as the nonconservativeness parameter.

The governing differential equation of the system can be derived from the extended form of Hamilton's principle:

$$\int_{t_1}^{t_2} \delta(T - \Phi + W_c)\,\mathrm{d}t + \int_{t_1}^{t_2} \delta W_{nc}\,\mathrm{d}t = 0, \tag{1}$$

where $T$ and $\Phi$ are the kinetic and elastic potential energy of the beam, respectively, while $W_c$ and $\delta W_{nc}$ represent the conservative work and the nonconservative virtual work of the applied loads. The above potential and work terms take the following aspect:

$$T = \frac{1}{2}\int_0^L \mu A\left(\frac{\partial v(x,t)}{\partial t}\right)^2 \mathrm{d}x, \tag{2}$$

$$\Phi = \frac{1}{2}\int_0^L EI\left(\frac{\partial^2 v(x,t)}{\partial x^2}\right)^2 \mathrm{d}x, \tag{3}$$

$$W_c = \int_0^L N\frac{1}{2}\left(\frac{\partial v(x,t)}{\partial x}\right)^2 \mathrm{d}x, \tag{4}$$

where $N$ is the compressive axial force at a generic coordinate $x$, calculated as

$$N = \int_x^L q_\alpha\,\mathrm{d}x + P. \tag{5}$$

The transverse components of the follower forces are nonconservative for which any potential energy can be defined. The nonconservative virtual work of these transverse components can be expressed as

$$\begin{aligned}\delta W_{nc} &= -\int_0^L q_\alpha \sin(\alpha\varphi(x,t))\,\delta v(x,t)\,\mathrm{d}x - P\sin(\alpha\varphi(L,t))\,\delta v(L,t)\\ &= -\int_0^L q_\alpha \alpha\left(\frac{\partial v(x,t)}{\partial x}\right)\delta v(x,t)\,\mathrm{d}x - P\alpha\left(\frac{\partial v(L,t)}{\partial x}\right)\delta v(L,t).\end{aligned} \tag{6}$$

Taking the variations of the energy and work terms (2)–(4) and (6), and substituting them into the extended Hamilton's principle (1), yields

$$\begin{aligned}\int_{t_1}^{t_2}\Bigg\{\int_0^L\Bigg(&\mu A\left(\frac{\partial v}{\partial t}\right)\delta\left(\frac{\partial v}{\partial t}\right) - EI\left(\frac{\partial^2 v}{\partial x^2}\right)\delta\left(\frac{\partial^2 v}{\partial x^2}\right) + N\left(\frac{\partial v}{\partial x}\right)\delta\left(\frac{\partial v}{\partial x}\right)\\ &- q_\alpha\alpha\left(\frac{\partial v}{\partial x}\right)\delta v\Bigg)\mathrm{d}x - P\alpha\left(\frac{\partial v(L,t)}{\partial x}\right)\delta v(L,t)\Bigg\}\mathrm{d}t = 0,\end{aligned} \tag{7}$$

where $v$ has been used to indicate $v(x, t)$. Integrating by parts and considering that the variational formulation (7) must be valid for any interval of time, leads to

$$\begin{aligned}&\int_0^L(-\mu A\ddot{v} - EIv^{\mathrm{IV}} - 2(EI' + E'I)v''' - (EI'' + E''I + 2E'I')v'' - Nv'' - (\alpha-1)q_\alpha v')\delta v\,\mathrm{d}x\\ &- [EIv''\delta v']_0^L + [(Nv' + (EIv'')')\,\delta v]_0^L - [P\alpha v'\delta v]^L = 0,\end{aligned} \tag{8}$$

where the prime stands for partial derivative with respect to $x$, the overdot means partial derivative with respect to time $t$ and having considered that $N' = -q_\alpha$. Since the variations are arbitrary, their coefficients must vanish independently in order to make the entire expression (8) vanish. Therefore, the following field equation and boundary conditions are obtained:

$$\begin{aligned}&\mu A\ddot{v} + EIv^{\mathrm{IV}} + 2(EI' + E'I)v''' + (EI'' + E''I + 2E'I')v'' + Nv'' + (\alpha-1)q_\alpha v' = 0,\\ &[(Nv' + EIv''' + EI'v'' + E'Iv'')\delta v]_{x=0} = 0,\\ &[EIv''\delta v']_{x=0} = 0,\\ &[((N - P\alpha)v' + EIv''' + EI'v'' + E'Iv'')\delta v]_{x=L} = 0,\\ &[EIv''\delta v']_{x=L} = 0.\end{aligned} \tag{9}$$

Assuming a time harmonic form for the displacement

$$v(x,t) = V(x)\,\mathrm{e}^{\mathrm{i}\omega t}, \tag{10}$$

where $\omega$ is the circular frequency of vibration, and substituting into Eq. (9) leads to the final form of the differential governing field equation:

$$EIV^{\mathrm{IV}} + 2(EI' + E'I)V''' + (EI'' + E''I + 2E'I')V'' + NV'' + (\alpha-1)q_\alpha V' = \omega^2\mu AV \tag{11}$$

with the general static and kinematic boundary conditions:

$$\begin{aligned}&[(NV' + EIV''' + EI'V'' + E'IV'')\,\delta V]_{x=0} = 0,\\ &[EIV''\delta V']_{x=0} = 0,\\ &[((N - P\alpha)V' + EIV''' + EI'V'' + E'IV'')\delta V]_{x=L} = 0,\\ &[EIV''\delta V']_{x=L} = 0.\end{aligned} \tag{12}$$

## 3. GDQ methodology

In this section, the GDQ method is first reviewed and then applied to represent the governing differential field equation (11) and boundary conditions (12) as a set of algebraic equations defined at some discrete points.

### 3.1. GDQ review

The essence of the GDQ method is that the $n$th-order derivative of a smooth one-dimensional function $f(x)$ defined over the interval [0, $L$] at the $i$th point of abscissa $x_i$, can be approximated as

$$\left.\frac{\mathrm{d}^n f(x)}{\mathrm{d}x^n}\right|_{x=x_i} \cong \sum_{j=1}^{\mathcal{N}} \beta_{ij}^{(n)} f(x_j), \tag{13}$$

where $\beta_{ij}^{(n)}$ is the $n$th-order weighting coefficient at the $i$th point calculated for the $j$th sampling point of the domain. In Eq. (13) $\mathcal{N}$ is the total number of the sampling points of the grid distribution and $f(x_j)$ is the value of the function at the $j$th point.

Some simple recursive formulas are available for calculating $n$th-order derivative weighting coefficients $\beta_{ij}^{(n)}$ by means of Lagrange polynomial interpolation functions [10]. The weighting coefficients for the first-order derivative are

$$\beta_{ij}^{(1)} = \frac{\mathsf{L}^{(1)}(x_i)}{(x_i - x_j)\mathsf{L}^{(1)}(x_j)}, \quad i,j = 1,2,\ldots,\mathcal{N}, \quad i \neq j, \tag{14}$$

$$\beta_{ii}^{(1)} = -\sum_{j=1, j\neq i}^{\mathcal{N}} \beta_{ij}^{(1)}, \quad i,j = 1,2,\ldots,\mathcal{N}, \quad i = j. \tag{15}$$

In Eq. (14) the first derivative of Lagrange interpolating polynomials at each point $x_k$, $k = 1, ..., \mathcal{N}$, is

$$\mathsf{L}^{(1)}(x_k) = \prod_{l=1, l\neq k}^{\mathcal{N}} (x_k - x_l), \quad k = 1,\ldots,\mathcal{N}. \tag{16}$$

For higher order derivatives ($n = 2, 3, \ldots, \mathcal{N} - 1$), one gets iteratively

$$\beta_{ij}^{(n)} = n\left(\beta_{ii}^{(n-1)}\beta_{ij}^{(1)} - \frac{\beta_{ij}^{(n-1)}}{x_i - x_j}\right), \quad i,j = 1,2,\ldots,\mathcal{N}, \quad i \neq j, \tag{17}$$

$$\beta_{ii}^{(n)} = -\sum_{j=1, j\neq i}^{\mathcal{N}} \beta_{ij}^{(n)}, \quad i,j = 1,2,\ldots,\mathcal{N}, \quad i = j. \tag{18}$$

Throughout the paper, the Chebyshev–Gauss–Lobatto grid point's distribution (Fig. 2) is assumed, for which the coordinates of the grid points $x_i$ along the beam length are

$$x_i = \frac{L}{2}\left[1 - \cos\left(\frac{i-1}{\mathcal{N}-1}\pi\right)\right], \quad i = 1,2,\ldots,\mathcal{N}, \tag{19}$$

where $L$ is the length of the column.

It has been proven that for the Lagrange interpolating polynomials, the Chebyshev–Gauss–Lobatto sampling points rule guarantees convergence and efficiency to the GDQ technique [10–14].

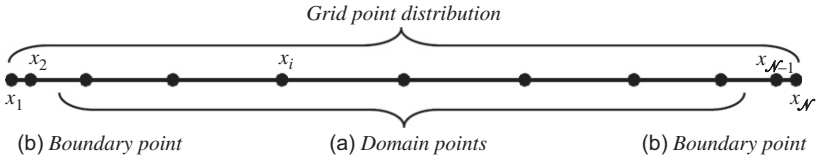


Fig. 2. Chebyshev–Gauss–Lobatto grid point distribution with $\mathcal{N} = 11$: (a) domain points and (b) boundary points.

### 3.2. Discrete governing equations

The numerical procedure illustrated above enables one to write the governing equation and boundary conditions in discrete form, transforming every space derivative into a weighted sum of nodal values. The general differential governing equation (11) is represented via GDQ technique at the $i = 3, 4, \ldots, \mathcal{N} - 2$ grid domain points (Fig. 2) as

$$\begin{aligned} &E_i I_i \sum_{j=1}^{\mathcal{N}} \beta_{ij}^{(4)} V_j + 2\left( E_i \sum_{j=1}^{\mathcal{N}} \beta_{ij}^{(1)} I_j + I_i \sum_{j=1}^{\mathcal{N}} \beta_{ij}^{(1)} E_j \right) \sum_{j=1}^{\mathcal{N}} \beta_{ij}^{(3)} V_j \\ &+ \left( E_i \sum_{j=1}^{\mathcal{N}} \beta_{ij}^{(2)} I_j + I_i \sum_{j=1}^{\mathcal{N}} \beta_{ij}^{(2)} E_j + 2 \sum_{j=1}^{\mathcal{N}} \beta_{ij}^{(1)} E_j \sum_{j=1}^{\mathcal{N}} \beta_{ij}^{(1)} I_j \right) \sum_{j=1}^{\mathcal{N}} \beta_{ij}^{(2)} V_j \\ &+ N_i \sum_{j=1}^{\mathcal{N}} \beta_{ij}^{(2)} V_j + (\alpha - 1) q_{\alpha i} \sum_{j=1}^{\mathcal{N}} \beta_{ij}^{(1)} V_j = \omega^2 \mu_i A_i V_i, \end{aligned} \tag{20}$$

where $\mu_i$, $E_i$, $A_i$, $I_i$, $N_i$, $q_{\alpha i}$ and $V_i$ indicate the mass density, Young's modulus, the cross-sectional area, the second moment of inertia, the axial force, the modulus of the subtangential force and the column deflection at the $i$th grid point of abscissa $x_i$, respectively. For a cantilever beam clamped at $x = 0$, the boundary conditions (12) can be expressed via GDQ approximation at the first grid point $i = 1$ as

$$\begin{aligned} &V_1 = 0, \\ &\sum_{j=1}^{\mathcal{N}} \beta_{1j}^{(1)} V_j = 0 \end{aligned} \tag{21}$$

and at the last $i = \mathcal{N}$ grid point ($x = L$) as

$$\begin{aligned} &(N_{\mathcal{N}} - P\alpha) \sum_{j=1}^{\mathcal{N}} \beta_{\mathcal{N}j}^{(1)} V_j + E_{\mathcal{N}} I_{\mathcal{N}} \sum_{j=1}^{\mathcal{N}} \beta_{\mathcal{N}j}^{(3)} V_j + \left( E_{\mathcal{N}} \sum_{j=1}^{\mathcal{N}} \beta_{\mathcal{N}j}^{(1)} I_j + I_{\mathcal{N}} \sum_{j=1}^{\mathcal{N}} \beta_{\mathcal{N}j}^{(1)} E_j \right) \sum_{j=1}^{\mathcal{N}} \beta_{\mathcal{N}j}^{(2)} V_j = 0, \\ &E_{\mathcal{N}} I_{\mathcal{N}} \sum_{j=1}^{\mathcal{N}} \beta_{\mathcal{N}j}^{(2)} V_j = 0. \end{aligned} \tag{22}$$

Note that in this case any discrete equation is formulated at the grid points $i = 2$ and $\mathcal{N} - 1$ [10]. Indicating more synthetically with

$$\left.\begin{aligned} \mathbf{K}_{ij}^{e} &= E_i I_i \beta_{ij}^{(4)} + 2\left( E_i \sum_{j=1}^{\mathcal{N}} \beta_{ij}^{(1)} I_j + I_i \sum_{j=1}^{\mathcal{N}} \beta_{ij}^{(1)} E_j \right) \beta_{ij}^{(3)} \\ &+ \left( E_i \sum_{j=1}^{\mathcal{N}} \beta_{ij}^{(2)} I_j + I_i \sum_{j=1}^{\mathcal{N}} \beta_{ij}^{(2)} E_j + 2 \sum_{j=1}^{\mathcal{N}} \beta_{ij}^{(1)} E_j \sum_{j=1}^{\mathcal{N}} \beta_{ij}^{(1)} I_j \right) \beta_{ij}^{(2)} \\ \mathbf{K}_{ij}^{g} &= N_i \beta_{ij}^{(2)}, \\ \mathbf{K}_{ij}^{nc} &= (\alpha - 1) q_{\alpha i} \beta_{ij}^{(1)}, \end{aligned}\right\} \quad \begin{aligned} i &= 3, 4, \ldots, \mathcal{N} - 2, \\ j &= 1, 2, \ldots, \mathcal{N}, \end{aligned} \tag{23}$$

the $(\mathcal{N} - 4) \times \mathcal{N}$ stiffness matrices and with

$$\mathbf{M}_d = \operatorname{diag}\begin{bmatrix} \mu_3 A_3 & \mu_4 A_4 & \cdots & \mu_{\mathcal{N}-3} A_{\mathcal{N}-3} & \mu_{\mathcal{N}-2} A_{\mathcal{N}-2} \end{bmatrix} \tag{24}$$

the $(\mathcal{N} - 4) \times (\mathcal{N} - 4)$ mass matrix, the $\mathcal{N} - 4$ field equations defined by Eq. (20) can also be written in matrix form as

$$\mathbf{K}_d \boldsymbol{\delta} = \omega^2 \mathbf{M} \boldsymbol{\delta}_d. \tag{25}$$

In Eq. (25) the stiffness matrix $\mathbf{K}_d = \mathbf{K}^e + \mathbf{K}^g + \mathbf{K}^{nc}$ is the sum of the elastic stiffness properties of the beam defined by the matrix $\mathbf{K}^e$, the geometric stiffness contribute $\mathbf{K}^g$ induced by the conservative load and the nonconservativeness stiffness of the beam $\mathbf{K}^{nc}$ related to the nonconservative loads.

Also, in Eq. (25) $\boldsymbol{\delta} = \begin{bmatrix} V_1 & V_2 & \cdots & V_{\mathscr{N}-1} & V_{\mathscr{N}} \end{bmatrix}^{\mathrm{T}}$ is the $\mathscr{N} \times 1$ vector of unknown displacements at the grid points, while $\boldsymbol{\delta}_d = \begin{bmatrix} V_3 & V_4 & \cdots & V_{\mathscr{N}-4} & V_{\mathscr{N}-3} \end{bmatrix}^{\mathrm{T}}$ collects only the $(\mathscr{N}-4) \times 1$ unknown displacements at the domain points.

The four boundary conditions described in Eqs. (21) and (22) are also written in synthetic vector notation as

$$\mathbf{K}_b \boldsymbol{\delta} = \mathbf{0}, \tag{26}$$

where the $4 \times \mathscr{N}$ matrix $\mathbf{K}_b$ is defined as

$$\mathbf{K}_b = \begin{bmatrix} 1 & 0 & \cdots & 0 & 0 \\ \beta_{11}^{(1)} & \beta_{12}^{(1)} & \cdots & \beta_{1(\mathscr{N}-1)}^{(1)} & \beta_{1\mathscr{N}}^{(1)} \\ k_{\mathscr{N}1} & k_{\mathscr{N}2} & \cdots & k_{\mathscr{N}(\mathscr{N}-1)} & k_{\mathscr{N}\mathscr{N}} \\ E_{\mathscr{N}} I_{\mathscr{N}} \beta_{\mathscr{N}1}^{(2)} & E_{\mathscr{N}} I_{\mathscr{N}} \beta_{\mathscr{N}2}^{(2)} & \cdots & E_{\mathscr{N}} I_{\mathscr{N}} \beta_{\mathscr{N}(\mathscr{N}-1)}^{(2)} & E_{\mathscr{N}} I_{\mathscr{N}} \beta_{\mathscr{N}\mathscr{N}}^{(2)} \end{bmatrix} \tag{27}$$

and where the $j$th $k_{\mathscr{N}j}$ coefficient is defined as

$$k_{\mathscr{N}j} = (N_{\mathscr{N}} - P\alpha)\beta_{\mathscr{N}j}^{(1)} + E_{\mathscr{N}} I_{\mathscr{N}} \beta_{\mathscr{N}j}^{(3)} + \left( E_{\mathscr{N}} \sum_{j=1}^{\mathscr{N}} \beta_{\mathscr{N}j}^{(1)} I_j \right) \beta_{\mathscr{N}j}^{(2)} + \left( I_{\mathscr{N}} \sum_{j=1}^{\mathscr{N}} \beta_{\mathscr{N}j}^{(1)} E_j \right) \beta_{\mathscr{N}j}^{(2)}. \tag{28}$$

The discrete field and boundary conditions can be collected as $\mathscr{N}$ algebraic equations in the $\mathscr{N}$ unknowns nodal displacements as

$$\begin{bmatrix} \mathbf{K}_b \\ \mathbf{K}_d \end{bmatrix} \boldsymbol{\delta} = \begin{bmatrix} \mathbf{0} \\ \omega^2 \mathbf{M}_d \boldsymbol{\delta}_d \end{bmatrix}. \tag{29}$$

In order to calculate the natural frequencies of the structure, Eq. (29) need to be reorganized in the following form:

$$\begin{bmatrix} \mathbf{K}_{bb} & \mathbf{K}_{bd} \\ \mathbf{K}_{db} & \mathbf{K}_{dd} \end{bmatrix} \begin{bmatrix} \boldsymbol{\delta}_b \\ \boldsymbol{\delta}_d \end{bmatrix} = \omega^2 \begin{bmatrix} \mathbf{0} & \mathbf{0} \\ \mathbf{0} & \mathbf{M}_d \end{bmatrix} \begin{bmatrix} \boldsymbol{\delta}_b \\ \boldsymbol{\delta}_d \end{bmatrix}, \tag{30}$$

where the subscripts $b$ and $d$, refer to the system degrees of freedom at the boundaries and in the beam domain (Fig. 2), respectively, and $\boldsymbol{\delta}_b = \begin{bmatrix} V_1 & V_2 & V_{\mathscr{N}-1} & V_{\mathscr{N}} \end{bmatrix}^{\mathrm{T}}$. Kinematical condensation of the nondomain degrees of freedom leads to the final equation for the computation of the system eigenfrequency:

$$(\mathbf{K}_{dd} - \mathbf{K}_{db} \mathbf{K}_{bb}^{-1} \mathbf{K}_{bd}) \boldsymbol{\delta}_d = \omega^2 \mathbf{M}_d \boldsymbol{\delta}_d. \tag{31}$$

## 4. Application to some known nonconservative problems

In this section, Beck's column problem, Leipholz's column problem and Hauger's column problem are studied. All these cases are characterized by a uniform cross-section column and clamped-free boundary conditions. It follows that the elastic stiffness matrix $\mathbf{K}^e$ and mass matrix $\mathbf{M}_d$ are identical for all cases, while the geometric $\mathbf{K}^g$ and nonconservative $\mathbf{K}^{nc}$ stiffness matrices as well the boundary conditions vary and can be derived from Eqs. (23) and (27) by simply setting the specific load conditions.

### 4.1. Beck's column

Beck's column problem consists in a slender cantilever beam of uniform cross-section, clamped at the base ($x = 0$) and loaded by a compressive concentrated follower force, $P$, acting at the top of the beam ($x = L$),

as shown in Fig. 3(a). Based on Eq. (5), the column is subjected to a constant compressive axial force $N(x) = P$. Therefore, in this case the values of $A_i$, $I_i$, $\mu_i$, $E_i$, and $N_i$ are the same at the grid points. The nonconservative matrix $\mathbf{K}^{nc}$ is null because $q_\alpha(x)$ is zero and the nonconservativeness of the system is retained by the third boundary condition only.

In Fig. 4 are represented the eigenfrequency curves for Beck's column in terms of dimensionless load $Q_B = PL^2/EI$ and eigenfrequency $\Omega = \sqrt{\mu AL^4\omega^2/EI}$ parameters, obtained by using a Chebyshev–Gauss–Lobatto grid distribution with 51 points. In addition to the case treated by Beck, for which $\alpha = 1.0$, the cases for $\alpha = 0.0, 0.1, \ldots, 0.9$ are also represented.

For $P = 0$ the first two natural frequencies of the unloaded column are obtained. For increasing magnitude of the load the second eigenfrequency $\Omega_2$ of the system is always decreasing while the first eigenfrequency $\Omega_1$ may rise or decrease depending on the value of the nonconservativeness parameter $\alpha$. This leads to both type of instability: divergence and flutter. In particular, Beck's column loses its stability via divergence for $\alpha \leqslant 0.4$, for which the $\Omega_1$ branches reach zero frequency at the critical divergence load points, and by flutter for $\alpha \geqslant 0.6$, where the $\Omega_1$ and $\Omega_2$ branches approach each other becoming coincident at the critical flutter load points. As confirmed by Rao and Rao [19] by an exact analysis, for $\alpha$ approaching the value of 0.5 Beck's column might be instable for divergence ($\alpha \to 0.5^-$) or flutter ($\alpha \to 0.5^+$) with two distinct values of the critical load. Therefore the value $\alpha = 0.5$ denotes the edge between the divergence and flutter instability for Beck's problem signing the limit of applicability of the static criterion in the stability study. It should be noted that, while the critical load

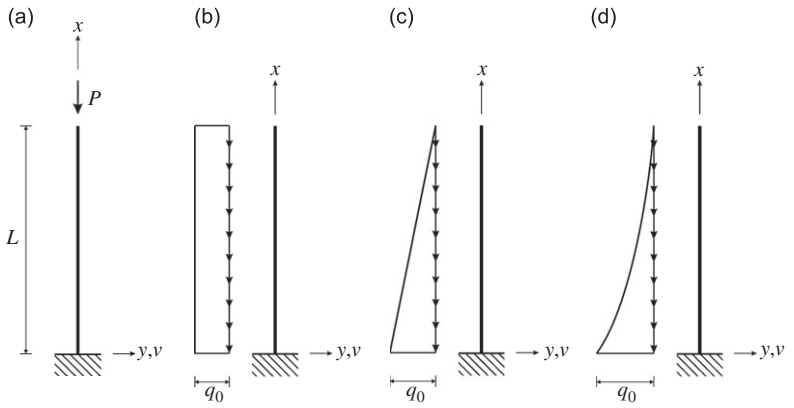


Fig. 3. (a) Beck's problem, (b) Leipholz's problem, (c) Hauger's problem and (d) Cantilever beam with quadratic distribution of the subtangential forces.

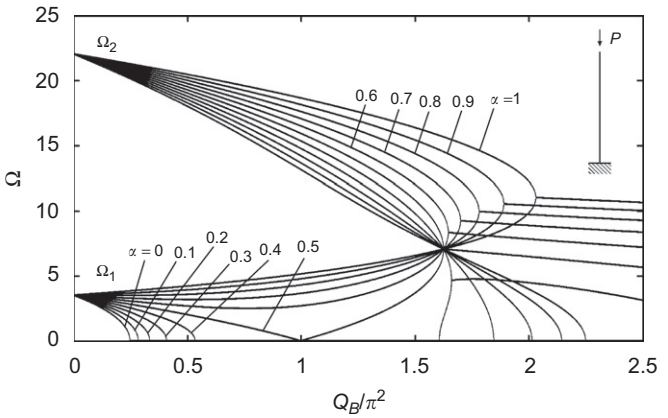


Fig. 4. Eigenfrequency curves for Beck's column for various values of the nonconservative parameter $\alpha$.

Table 1
Critical loads $Q_{B_{cr}}$ for the Beck's column for various values of the nonconservativeness parameter $\alpha$

| $\alpha$ | [19] | [20] | [21] | [22] | GDQ[a] |
|---|---|---|---|---|---|
| 0.0 | 2.4674 | 2.4674 | 2.4674 | | 2.4675 |
| 0.1 | 2.8296 | 2.830 | 2.830 | | 2.8296 |
| 0.2 | 3.3251 | 3.325 | 3.325 | | 3.3251 |
| 0.3 | 4.0550 | 4.055 | 4.055 | | 4.0551 |
| 0.4 | 5.2924 | 5.292 | 5.293 | | 5.2925 |
| 0.5 | 9.8696, 16.0524 | 9.870 | 9.872 | | 9.8700, 16.0525 |
| 0.6 | – | – | 16.27 | | 16.2590 |
| 0.7 | – | – | 16.80 | 16.78750 | 16.7875 |
| 0.8 | – | – | 17.60 | 17.58923 | 17.5891 |
| 0.9 | – | – | 18.68 | 18.66848 | 18.6684 |
| 1.0 | – | 20.05 | 20.07 | 20.05102 | 20.05095 |

[a]Results obtained by the proposed formulation using a 51 points Chebyshev–Gauss–Lobatto grid distribution.

for divergence can be found by a static criterion, the flutter load can only be obtained by approaching the problem dynamically.

It can be observed from Fig. 4 that the critical load, either for divergence or flutter, increases for increasing values of $\alpha$ from 0 to 1, and so the pure conservative case ($\alpha = 0$) is the more susceptible of instability.

In Table 1 the GDQ critical loads are compared with the solutions obtained by Leipholz [20] through a classical Galerkin method, with those proposed by Kikuchi [21] via a finite element technique, and with the exact solutions given by Rao and Rao [19]. It can be seen that the GDQ results well approximate the exact solutions for $0.0 \leqslant \alpha \leqslant 0.4$.

At $\alpha = 0.5$, the GDQ solution becomes unstable when the $\Omega_1$ eigenfrequency branch is approaching zero value. In particular, the $\Omega_1$ eigenfrequency branch presents an oscillating behaviour crossing the zero frequency axis several times, so that the critical divergence load cannot be distinctively determined. The divergent critical load for $\alpha = 0.5$ given in Table 1, $Q_{B_{cr}} = 9.8700$, has been obtained as the load corresponding to the minimum of the 10th-order polynomial used to interpolate the nonsmooth oscillating curve.

For a pure follower force, $\alpha = 1.0$ (Beck's problem), the present formulation calculates the critical flutter load as $Q_{B_{cr}} = 20.0509$. This value is very close to the one given by Beck, i.e. $Q_{B_{cr}} = 20.051$, proving the accuracy of the GDQ method versus other numerical techniques. For example, Elfelsoufi and Azrar [23], by using a basis of polynomial functions and 60 points to discretize the domain, recently estimated Beck's critical load with a poorer approximation (i.e. $Q_{B_{cr}} = 20.0625$) if compared to the present formulation.

### 4.2. Leipholz's column

Leipholz's column problem, as shown in Fig. 3(b), consists in a uniform cantilever beam clamped at $x = 0$ and loaded by a uniform distribution of compressive subtangential forces $q_\alpha(x_i) = q_0$ (the tip force $P = 0$). By using Eq. (5), the axial force at the $i$th grid point of coordinate $x_i$ results $N(x_i) = q_0(L - x_i)$. The eigenfrequency curves for Leipholz's column represented in Fig. 5 are obtained by the proposed formulation using a Chebyshev–Gauss–Lobatto grid with 51 points. The dimensionless load parameter in this case is assumed as $Q_L = q_0 L^3/EI$ while the eigenfrequency parameter is the same as defined in the previous case. It can be seen that for increasing load magnitude, while the first eigenfrequency $\Omega_1$ might decrease or increase by varying the nonconservativeness parameter, the second eigenfrequency $\Omega_2$ is always decreasing and slightly influenced by the different values of $\alpha$. The system is unstable for divergence when $\alpha < 0.5$ and for flutter for $\alpha > 0.5$. Also for Leipholz's column the case $\alpha = 0.5$ denotes the separation between divergence and flutter instability. In fact, for $\alpha = 0.5$ the $\Omega_1$ eigenfrequency curve becomes unstable while approaching zero frequency value. In line with Beck's example, it can be assumed that approaching this value of the nonconservativeness of the applied loads the system presents the two different forms of instability with two different critical values. The divergence critical load for $\alpha \leqslant 0.5$ can be obtained via static criterion while the critical flutter load for $\alpha \geqslant 0.5$ can only be calculated by means of the dynamic approach.

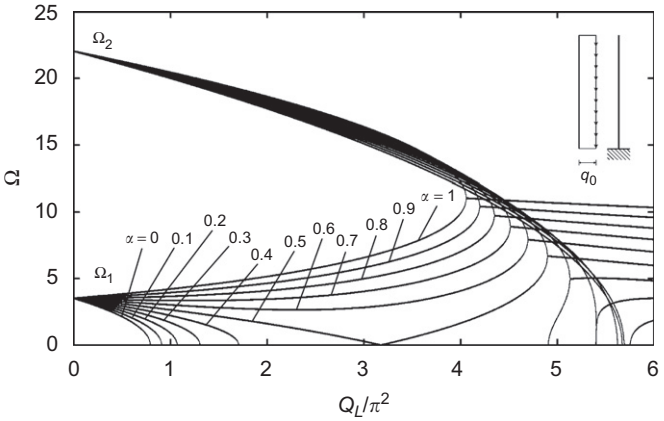


Fig. 5. Eigenfrequency curves for Leipholz's column for various values of the nonconservative parameter α.

By observing the eigenfrequency curves of Fig. 5 it can be seen that the critical load is not strictly monotonic for increasing α, as seen for Beck's problem. In fact, divergence load increases for increasing values of the parameter α from 0.0 to 0.5, while the critical flutter load decreases for increasing α from 0.6 to 1.0. The maximum critical load for this system correspond to the flutter load for $\alpha = 0.5$.

For $\alpha = 1.0$ the critical GDQ flutter load, $Q_{L_{cr}} = 40.0537$, compares extremely well with the solution $Q_{L_{cr}} = 40.05$ found by Leipholz [6]. In addition, this result is competitive if compared with other approximate solutions as specified in Ref. [24]: for example, the Galerkin solution by Leipholz yielded $Q_{L_{cr}} = 40.7$, the finite difference solution by Leipholz yielded $Q_{L_{cr}} = 38.6$, the one of Sugiyama et al. gave $Q_{L_{cr}} = 39.2$, Hauger reported a value of $Q_{L_{cr}} = 40.7$ and Elishakoff reported $Q_{L_{cr}} = 41.206$.

### 4.3. Haugher's column

Hauger's column model consists in a uniform cantilever beam clamped at $x = 0$ and loaded by a triangular distribution of compressive subtangential forces, $q_\alpha(x) = q_0(L - x)$, as shown in Fig. 3(c). The internal axial force at the generic grid point of abscissa $x_i$ is $N(x_i) = q_0(L - x_i)^2/2$. The eigenfrequency curves represented in Fig. 6 for α ranging from 0.0 to 1.0 are obtained by using a Chebyshev–Gauss–Lobatto grid with 51 points. The dimensionless load parameter is assumed as $Q_H = q_0 L^4/EI$ while the dimensionless frequency parameter is the same as defined above. The stability behaviour of this column is similar to the one of Leipholz's column, for which the maximum critical load is reached for $\alpha = 0.5$ when the system is unstable for flutter. The eigenfrequency curves in Fig. 6 are coincident with those obtained via a displacement-based finite element formulation by Ryu et al. [25] and later by two of the authors [26].

In the case of $\alpha = 1.0$, the GDQ flutter load for Hauger's column $Q_{H_{cr}} = 150.6416$ is presented in Table 2 along with those calculated for Beck's and Leipholz's column and with those of several referenced papers. The table shows clearly the accuracy of the GDQ method in the calculation of the critical flutter load ($\alpha = 1.0$) for the three classical stability problems considered.

### 4.4. Study on procedure convergence and different boundary conditions

In order to investigate the GDQ procedure convergence, the critical flutter load for the three classical problems in the case $\alpha = 1.0$ was investigated by varying the number of grid points. Results are collected in Table 3 increasing the number of points of the Chebyshev–Gauss–Lobatto grid distribution from 13 up to 51. It can be seen that the proposed GDQ formulation well captures the dynamic behaviour of the system for flutter instability by using only 21 points, for which the errors on the critical flutter loads with the respect to the exact values are smaller than the 0.1%. It can also be seen that for all the considered systems, the formulation is stable while increasing the number of points and that the use of 51 points guarantees convergence of the procedure.

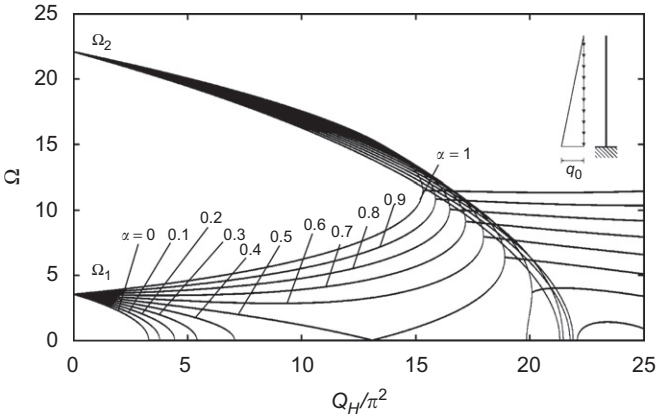


Fig. 6. Eigenfrequency curves for Hauger's column for various values of the nonconservative parameter α.

Table 2
Comparison of critical load for the Beck's, Leipholz's and Hauger's column ($\alpha = 1.0$)

| Author—year—reference | $\alpha = 1.0$ | | |
|---|---|---|---|
| | $Q_{B_{cr}}$ | $Q_{L_{cr}}$ | $Q_{H_{cr}}$ |
| Beck—1952—[2] | 20.051 | – | – |
| Leipholz—1962—[28] | – | 40.70 | – |
| Hauger—1966—[29] | – | – | 158.20 |
| Stability Handbook—1971—[30] | 20.05 | 40.70 | 158.20 |
| Rao and Rao—1975—[22] | 20.05102 | 40.05376 | 150.64225 |
| Leipholz—1980—[6] | 20.30 | 40.05 | 150.80 |
| De Rosa and Franciosi—1990—[31] | 20.05 | 40.05 | 150.20 |
| Glabisz—1993—[32] | 20.05095 | 40.0537 | 150.6415 |
| Katsikadelis—2007—[33] | 20.06 | 40.08 | 150.75 |
| GDQ[a] | 20.05095 | 40.05374 | 150.6416 |

[a]Results obtained by the proposed formulation using a 51 points Chebyshev–Gauss–Lobatto grid distribution.

Table 3
Critical load for the Beck's, Leipholz's and Hauger's column for an increasing the number of grid points $\mathcal{N}$ of the Chebyshev–Gauss–Lobatto distribution

| Number of points $\mathcal{N}$ | Beck | Leipholz | Hauger |
|---|---|---|---|
| | $Q_{B_{cr}}$ $(\alpha = 1.0)$ | $Q_{L_{cr}}$ $(\alpha = 1.0)$ | $Q_{H_{cr}}$ $(\alpha = 1.0)$ |
| 13 | 22.14198 | 42.33998 | 152.86992 |
| 17 | 20.23291 | 40.23906 | 150.7663 |
| 21 | 20.06358 | 40.0665 | 150.65013 |
| 25 | 20.05168 | 40.05447 | 150.64211 |
| 29 | 20.05099 | 40.05378 | 150.64163 |
| 31 | 20.05097 | 40.05375 | 150.64161 |
| 51 | 20.05095 | 40.05374 | 150.6416 |

The proposed GDQ formulation has also been applied to others boundary conditions, namely the pinned–pinned beam, the clamped–pinned beam and the clamped–clamped beam. In Table 4 only a numerical comparison of the GDQ critical loads for $\alpha = 1.0$ with some literature results is presented. An extensive

Table 4
Critical load for the pinned–pinned, clamped–pinned and clamped–clamped beam subjected to Beck's, Leipholz's and Hauger's columns ($\alpha = 1.0$)

| Author—year—reference | $\alpha = 1.0$ | | | | | | | | |
|---|---|---|---|---|---|---|---|---|---|
| | Pinned–pinned | | | Clamped–pinned | | | Clamped–clamped | | |
| | $Q_{B_{cr}}$ | $Q_{L_{cr}}$ | $Q_{H_{cr}}$ | $Q_{B_{cr}}$ | $Q_{L_{cr}}$ | $Q_{H_{cr}}$ | $Q_{B_{cr}}$ | $Q_{L_{cr}}$ | $Q_{H_{cr}}$ |
| Hauger—1966—[29] | – | 18.96 | 62.28 | – | 57.95 | 402.3 | – | 81.37 | 328.0 |
| Stability Handbook—1971—[30] | 9.87 | 18.96 | 62.68 | 20.20 | 57.95 | 402.3 | 39.50 | 81.37 | 328.00 |
| Leipholz and Bhalla—1977—[34] | – | – | 61.866 | – | – | 313.6 | – | – | 375.2 |
| Leipholz—1980—[6] | – | 18.96 | 61.866 | – | 57.00 | 313.6 | – | 80.26 | 375.2 |
| Sugiyama and Mladenov—1983—[35] | – | – | 61.866 | – | – | 313.49 | – | – | 375.01 |
| De Rosa and Franciosi—1990—[31] | – | – | 61.85 | – | – | 312.22 | – | – | 373.1 |
| Ryu et al.—2000—[25] | – | – | 61.95 | – | – | 313.82 | – | – | 375.35 |
| GDQ[a] | 9.8697 | 18.9563 | 61.8667 | 20.1363 | 57.0077 | 313.5038 | 39.4785 | 80.2558 | 375.0196 |

[a]Results obtained by the proposed formulation using a 51 points Chebyshev–Gauss–Lobatto grid distribution.

discussion on the boundary conditions effect on the stability of conservative and nonconservative loaded columns was given by two of the authors in a previous work [27].

## 5. Nonclassical stability problems

In this section, the unified discretized GDQ equation is characterized for four different nonclassical nonconservative stability problems. First, a uniform cantilever column subjected to a quadratic distribution of subtangential forces is studied. Next, a linear and a quadratic tapered cantilever beam under a compressive concentrated subtangential force acting at the top of the beams are investigated. Finally, a linear tapered circular beam with varying material properties along the beam length is considered.

In the previous section it has been shown that for the uniform beam problem the divergence type instability occurs for a zero value of the lowest eigenfrequency $\omega_1 = 0$, while the flutter-type instability takes place when the two lowest eigenfrequencies, $\omega_1$ and $\omega_2$, meet each other becoming complex conjugate. In this section, as well known, it is shown that flutter for tapered beams can take place for higher frequencies with respect to the first lowest two.

In each case investigated, the parametrical study for $\alpha$ varying from zero to one was carried out by adopting a Chebyshev–Gauss–Lobatto spatial grid with 51 points.

### 5.1. Cantilever beam with quadratic distribution of subtangential forces

A uniform cantilever beam clamped at $x = 0$ is considered subjected to a quadratic distribution of subtangential forces $q_\alpha(x) = q_0(L - x)^2$ and zero concentrated tip force $P = 0$, as shown in Fig. 3(d). The axial load at the grid point of abscissa $x_i$ is $N(x_i) = q_0(L - x_i)^3/3$. The discrete governing equation can be obtained from the general relations equation (30) by simply specifying the axial force and the nonconservativeness parameter. In Fig. 7 the eigenfrequency curves are represented for $\alpha$ varying from 0.0 to 1.0 in terms of the dimensionless load parameter $Q_Q = q_0 L^5/EI$ and the usual dimensionless frequency parameter.

It can be noted that the stability curves are similar to those of Leipholz's and Hauger's problems. The value $\alpha = 0.5$ denotes the limit between divergence and flutter instability. Compared to Leipholz's and Hauger's cases, it can be seen that the minimum critical flutter load is not realized for $\alpha = 1.0$ but for a smaller amount of the nonconservativeness of the applied loads.

Boris Shvartsman [36] has observed that for Beck's, Leipholz's and Hauger's column problems the critical divergence load for $\alpha = 0.5$ is always four times bigger than the critical load for conservative loaded system, i.e. $\alpha = 0.0$, as reported in the first three rows of Table 5. It should be noted that this consideration holds also

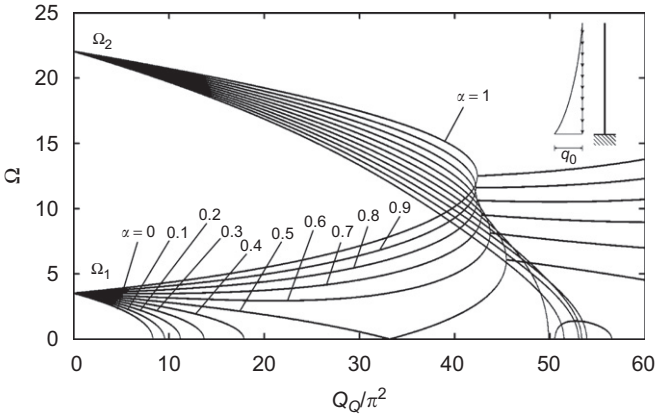


Fig. 7. Eigenfrequency curves for a straight uniform column subjected to a quadratic distribution of subtangential forces $q_x(x) = q_0(L-x)^2$ for various values of the nonconservative parameter $\alpha$.

Table 5
Critical divergence loads of the uniform beam for $\alpha = 0.0$ and 0.5 obtained by using a Chebyshev–Gauss–Lobatto grid distribution with 51 points

| Load case | Critical load $\alpha = 0.0$ | Critical load $\alpha = 0.5$ |
|---|---|---|
| $P(L)$ | 2.4675 | 9.8700 |
| $q_x(x) = q_0$ | 7.8374 | 31.3458 |
| $q_x(x) = q_0(L-x)$ | 32.2020 | 128.8180 |
| $q_x(x) = q_0(L-x)^2$ | 81.7708 | 327.0843 |

for the case under consideration, as shown in the last row of Table 5. This interesting result was not proven mathematically and might be a subject for a further study.

### 5.2. Linear tapered circular beam

Let us consider here a linear circular tapered cantilever beam of length $L$ clamped at $x = 0$. The beam is considered subjected to a concentrated compressive subtangential load $P$ at $x = L$, as shown in Fig. 8(a). The radius of the beam varies as follows:

$$r(x) = r_L\left[1 + \eta\left(1 - \frac{x}{L}\right)\right], \tag{32}$$

where $r_L = r(L)$ is the radius of the circular cross-section at the top of the beam, i.e. for $x = L$, and $\eta$ is the geometrical tapered parameter. For a null value of the tapered parameter, the uniform column is represented. For a tapered parameter $\eta = 1.0$ the beam radius at $x = 0$ is twice the radius at $x = L$. The constant axial load at the grid points is $N(x_i) = P$. Once the beam cross-sectional area $A_i = A(x_i)$ and moment of inertia $I_i = I(x_i)$ at the grid points are calculated, the discrete field and boundary governing equations are easily obtained. In Fig. 8(b)–(d) the eigenfrequency curves are presented for three different values of the tapered parameter, namely $\eta = 0.5$ in Fig. 8(b), $\eta = 1.0$ in Fig. 8(c) and $\eta = 1.5$ in Fig. 8(d). The dimensionless load parameter is assumed in this case as $Q_{BT} = PL^2/EI_L$, where $I_L$ is the moment of inertia of the cross-section at $x = L$. The critical loads for $\alpha = 0.0$, 0.2, 0.4, 0.6, 0.8 and 1.0 and for the different values of the tapered parameter are collected in Table 6.

Obviously, for fixed properties of the right-hand side of the beam ($x = L$), increasing values of the tapered parameter results in bigger natural frequencies as well as critical loads, as it can be seen by comparing the plots in Fig. 8(b)–(d) and numerically from Table 6. It is interesting to note from Fig. 8 that the divergence instability range decreases for increasing tapered parameter. In fact, for $\eta = 0.5$ the column is unstable for

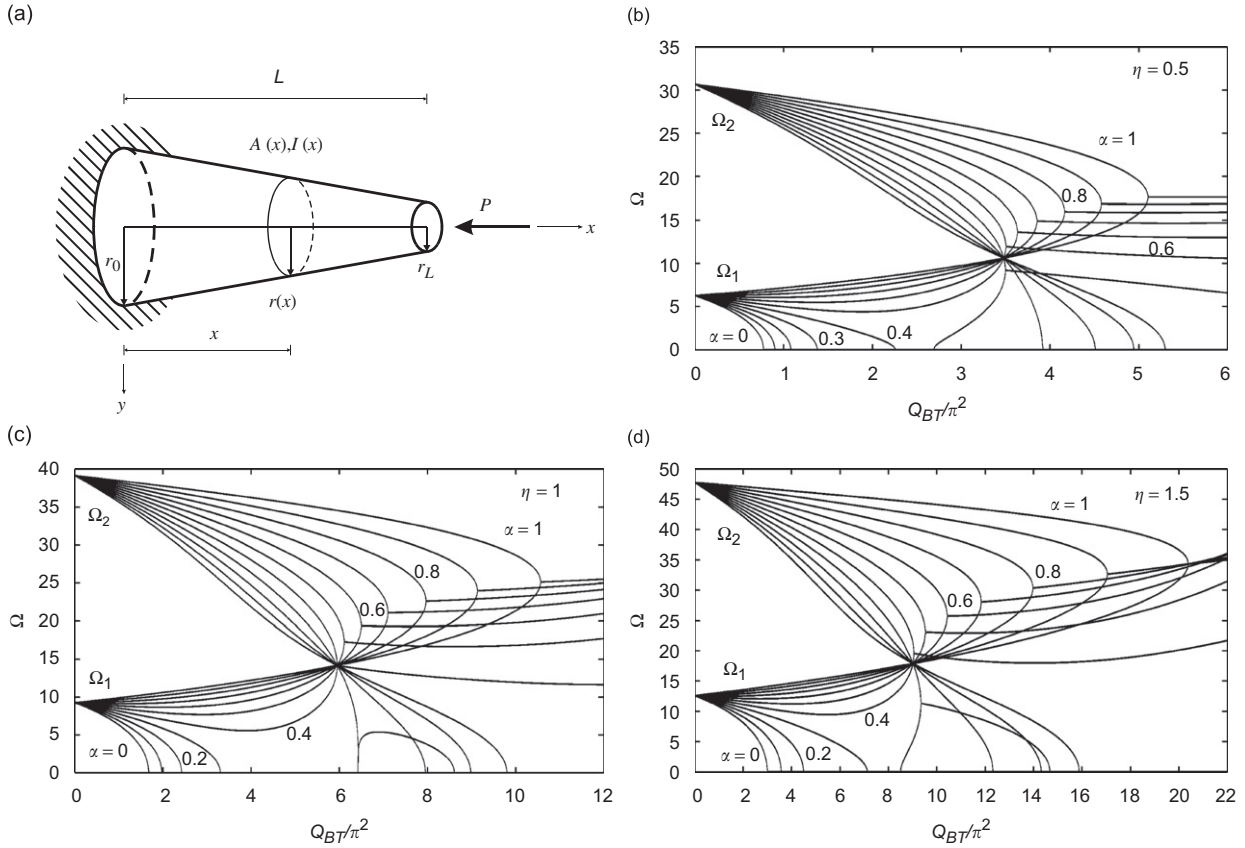


Fig. 8. (a) Linear tapered cantilever beam with circular cross-section subjected to a compressive concentrated subtangential force at $x = L$. Eigenfrequency curves for various values of the nonconservative parameter $\alpha$ in the case of (b) tapered parameter $\eta = 0.5$, (c) tapered parameter $\eta = 10$ and (d) tapered parameter $\eta = 1.5$.

Table 6
Critical load for the linear tapered $Q_{BT}$, symmetric tapered $Q_{BT}$ and Beck's $Q_{BM}$ columns for various values of the parameters $\eta$ and $\gamma$

| $\alpha$ | $Q_{BT}$ (linear) | | | $Q_{BT}$ (symmetric) | | | | | | $Q_{BM}$ |
|---|---|---|---|---|---|---|---|---|---|---|
| | $\eta = 0.5$ | $\eta = 1$ | $\eta = 1.5$ | $\eta = 0.5$ | $\eta = 1$ | $\eta = 1.5$ | $\eta = -0.5$ | $\eta = -1$ | $\eta = -1.5$ | $\gamma = 1$ |
| 0.0 | 7.5896 | 16.4639 | 29.5567 | 1.7122 | 1.0982 | 0.6334 | 3.3516 | 4.3465 | 5.4354 | 4.1245 |
| 0.2 | 10.6074 | 23.8276 | 44.2205 | 2.3048 | 1.4739 | 0.8451 | 4.5125 | 5.8397 | 7.2803 | 5.6359 |
| 0.4 | 22.2086 | 58.6041 | 89.2233 | 3.6554 | 2.3117 | 1.3031 | 7.1605 | 9.1661 | 11.3458 | 9.5147 |
| 0.6 | 35.7779 | 63.9863 | 102.7609 | 10.8766 | 6.9831 | 4.2356 | 23.5209 | 33.0862 | 45.465 | 23.4095 |
| 0.8 | 41.0242 | 78.4594 | 137.6707 | 11.429 | 7.1323 | 4.2171 | 26.1774 | 37.8375 | 53.2937 | 26.1952 |
| 1 | 50.3313 | 104.0404 | 200.9007 | 12.6084 | 7.6137 | 4.3696 | 30.7456 | 45.5436 | 65.2767 | 31.253 |

Results obtained by the proposed formulation using a 51 points Chebyshev–Gauss–Lobatto grid distribution.

divergence when $\alpha \leqslant 0.4$ while for $\eta = 1.5$ divergence appears only when $\alpha \leqslant 0.3$. This can be attributed to the shape effect that reduces the possibility for divergence instability for increasing values of the tapered parameters.

In particular in Fig. 9, the eigenfrequency curves for $\eta = 2.0$ show that divergence appear only for $\alpha \leqslant 0.2$. It is remarkable to note that for $\alpha \geqslant 0.9$ flutter instability takes place because the second and third eigenfrequencies coalesce (dotted lines in Fig. 9), for a much bigger value of critical load if compared to the case of $\alpha = 0.8$. For $\alpha = 0.8$, in fact, the critical load parameter is $Q_{BT_{\mathrm{cr}}} \approx 25$ while for $\alpha = 0.9$ the critical

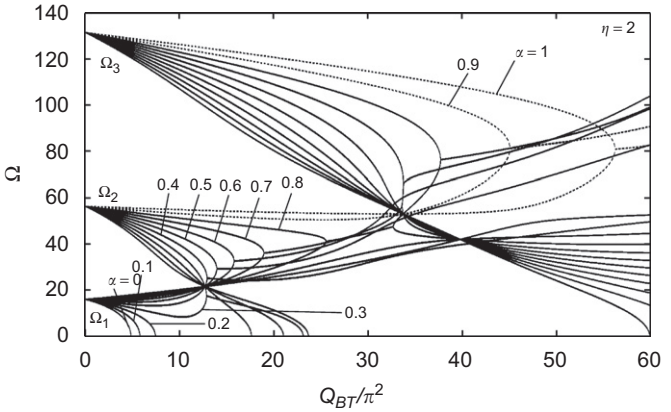


Fig. 9. Eigenfrequency curves for various values of the nonconservative parameter $\alpha$ for a linear tapered cantilever beam with circular cross-section subjected to a concentrated compressive subtangential force at $x = L$ for a tapered parameter $\eta = 2.0$.

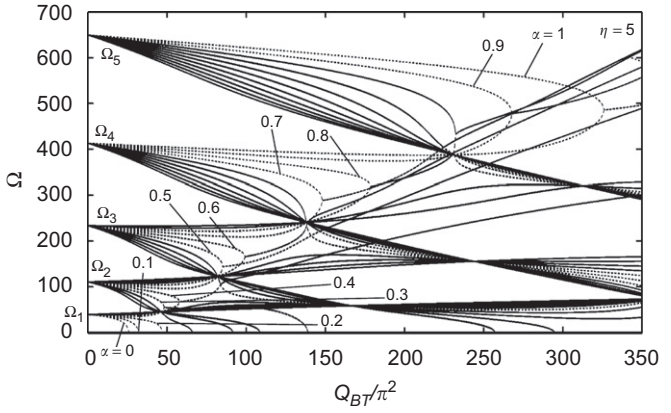


Fig. 10. Eigenfrequency curves for various values of the nonconservative parameter $\alpha$ for a linear tapered cantilever beam with circular cross-section subjected to a concentrated compressive subtangential force at $x = L$ for a tapered parameter $\eta = 5.0$.

flutter load jumps at $Q_{BT_{\rm cr}} \approx 45$. The shape effect can thus be important in the design with respect to the system critical flutter load. It has been shown, in a earlier work of two of the authors [37], that a similar behaviour happens in plates subjected to nonconservative subtangential forces for certain ratios of the plate dimensions.

It should be noted that by increasing further the tapered parameter flutter exists because the third and fourth eigenfrequencies coalesce for some values of the nonconservativeness parameter, and so on. For example in Fig. 10, where $\eta = 5.0$, it can be noted that for increasing values of $\alpha$, flutter takes place because higher frequencies coalesce with a great benefit of the system critical load. For instance, at $\alpha = 0.8$ the critical flutter load is $Q_{BT_{\rm cr}} \approx 175$ while for $\alpha = 0.9$ it reaches approximately the value $Q_{BT_{\rm cr}} \approx 275$.

### 5.3. Symmetric tapered circular beam

Here a column of length $L$ clamped at $x = 0$ and subjected to a concentrated compressive subtangential force at the beam's end is considered. The internal axial load at the grid points is $N(x_i) = P$. The beam radius in this case is assumed as

$$r(x) = r_L\left[1 + \frac{\eta}{L^2}(x^2 - Lx)\right], \tag{33}$$

where $r_L = r(L)$ and $\eta$ is still a sort of tapered parameter. The radius of the beam circular cross-section at $x = 0$ and $L$ is equal to $r_L$. For $\eta = 0$ the uniform column is reproduced. For $\eta > 0$ the beam is characterized by a contraction of the cross-section dimension that is maximum at the mid-length of the beam and varies with quadratic law. When $\eta < 0$ instead, the cross-section increases with quadratic law from the ends to the mid-length of the beam. For a given tapered parameter, once the beam cross-section area $A_i = A(x_i)$ and moment of inertia $I_i = I(x_i)$ at the grid points have been calculated, the discrete governing equations are obtained. Results are represented in Fig. 11 for increasing values of the tapered parameter $\eta = 0.5, 1.0, 1.5$ and in Fig. 12 for decreasing values of the tapered parameter $\eta = -0.5, -1.0, -1.5$. The dimensionless load parameter, $Q_{BT}$, is the same defined in Section 5.2.

Beside the expected shift of the eigenfrequency curves in terms of frequency and critical load, it can be noted that the pattern of the eigenfrequency curves does not change much for changing values of the tapered parameter. All the six cases represented in Figs. 11 and 12 are unstable for divergence in the range $\alpha \leqslant 0.5$ and for flutter for $\alpha \geqslant 0.6$. From this results it can be stated that the column can reach flutter instability for $\alpha = 0.5$ only in the case of uniform beam, because even a slight symmetric tapered effect leads the case of $\alpha = 0.5$ to be instable for divergence. Therefore, it can be assumed that in real structures, where small shape imperfections are always present, flutter instability is never realized for $\alpha = 0.5$.

In most of the cases of Figs. 10 and 11 the maximum critical load is reached for $\alpha = 1.0$. With respect to the linear tapered case described in Section 5.2, it can be observed that these quadratic shape effect has less consequence in the design of beams against flutter instability. For the six values of the tapered parameter, critical loads for several values of the nonconservativeness parameter are collected in Table 6.

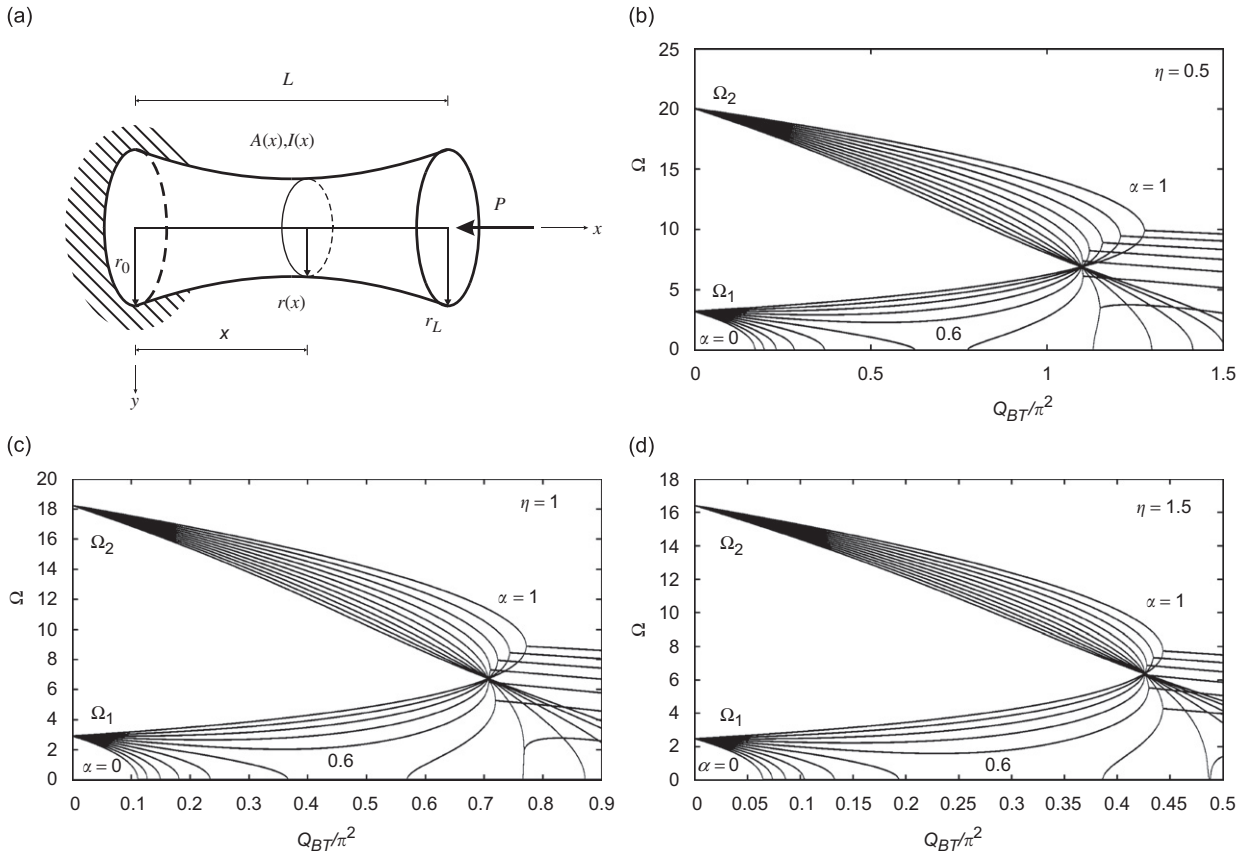


Fig. 11. (a) Symmetric tapered cantilever beam with circular cross-section subjected to a concentrated compressive subtangential force at $x = L$. Eigenfrequency curves for various values of the nonconservative parameter $\alpha$ and for (b) tapered parameter $\eta = 0.5$, (c) tapered parameter $\eta = 1.0$ and (d) tapered parameter $\eta = 1.5$.

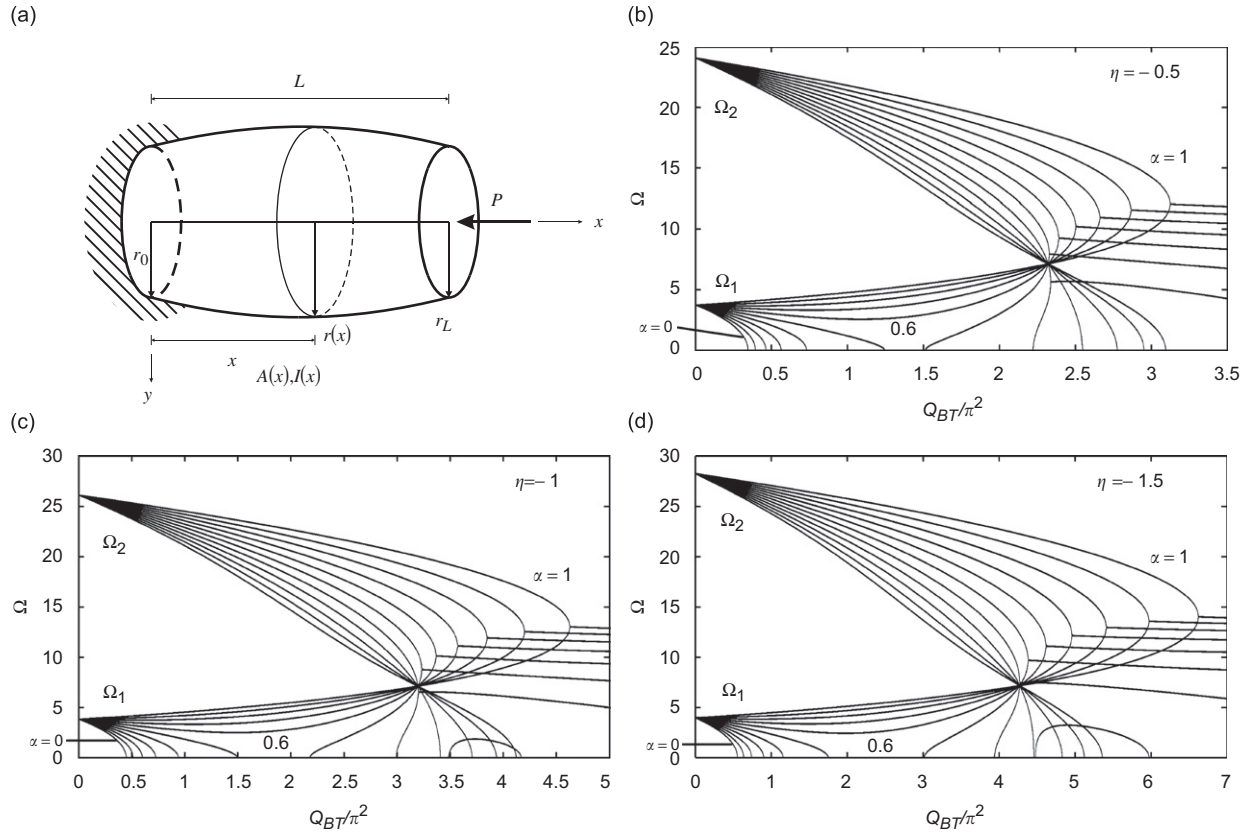


Fig. 12. (a) Symmetric tapered cantilever beam with circular cross-section subjected to a concentrated compressive subtangential force at $x = L$. Eigenfrequency curves for various values of the nonconservative parameter $\alpha$ and for (b) tapered parameter $\eta = -0.5$, (c) tapered parameter $\eta = -1.0$ and (d) tapered parameter $\eta = -1.5$.

### 5.4. Uniform beam with varying material properties

In this last example, a uniform cross-section cantilever beam with varying material properties along the beam length is considered. The beam, clamped at the bottom and free at the top, is subjected to a concentrated compressive subtangential force at the free end. In particular, it is considered that the modulus of elasticity $E(x)$ and the material density $\mu(x)$ of the beam at the generic abscissa $x$ can vary as

$$\mu(x) = \mu_L\left[1 + \gamma\left(1 - \frac{x}{L}\right)\right], \quad E(x) = E_L\left[1 + \gamma\left(1 - \frac{x}{L}\right)\right], \tag{34}$$

where $\mu_L = \mu(L)$, $E_L = E(L)$. The parameter $\gamma$ in Eq. (34) is thus used to define the amount of material properties variation between the bottom and top of the column.

In Fig. 13 the eigenfrequency curves for the case under consideration $\gamma = 1.0$ (continuous line) are overlapped with the solution for the uniform Beck's column $\gamma = 0$ (dashed line) presented in Fig. 3. Assuming the dimensionless load parameter as $Q_{BM} = PL^2/E_L I$, implies that at $x = 0.0$ the beam with $\gamma = 1.0$ has modulus of elasticity and material density twice of Beck's column. It is thus easy to note from Fig. 13 that increasing stiffness and material density of the column in proximity of its base (case $\gamma = 1.0$) induce a great benefit in the design against instability in terms of critical load. In addition, it can be seen that increasing the parameter $\gamma$ reduces the range for which the system may buckle for divergence. For example while Beck's problem (case $\gamma = 0.0$) undergoes divergence for values of $\alpha \leqslant 0.5$, only values of $\alpha \leqslant 0.4$ induce divergence in case of $\gamma = 1.0$. Critical load for the case of $\gamma = 1.0$ and for several values of $\alpha$ are finally summarized in Table 6.

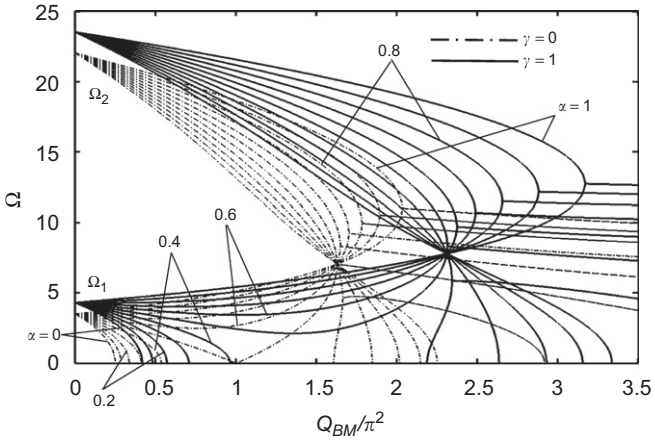


Fig. 13. Eigenfrequency curves for various values of the nonconservative parameter $\alpha$ for Beck's problem ($\gamma = 0$) in comparison with those obtained from a geometrical uniform beam subjected to a concentrated compressive subtangential force at $x = L$ with material tapered parameter $\gamma = 1$.

## 6. Comments and conclusions

In this paper, a GDQ-based algorithm for the determination of the frequencies of vibration of beams loaded by conservative and nonconservative forces is presented. First three classical stability problems have been used as benchmark cases to prove the reliability of the proposed approach. After that some nonclassical stability problems of tapered beams with geometrical varying properties have been investigated. Finally, the new aspect regarding the effect of variable mechanical properties on the stability of a uniform beam has been studied.

For the uniform beam problem the flutter-type instability takes place when the first two lowest eigenfrequencies coalesce. It is shown that for the nonuniform beam problem the flutter-type instability for certain values of the tapered parameter and nonconservativeness of the applied load may occur when the second and third eigenfrequencies meet each other becoming complex conjugate.

For each case a parametrical study for various values of the nonconservativeness of the applied load ($0.0 \leqslant \alpha \leqslant 1.0$) was performed and shown through the eigenfrequency curves.

For all the cases considered it has been noted that: the conservative loading condition ($\alpha = 0.0$) is the more susceptible of instability being associated with the lower critical load; the eigenfrequency value at which flutter takes place increases for increasing values of the nonconservativeness of the applied load. In the case of $\alpha = 1.0$, namely when purely nonconservative forces are applied to the systems, only flutter-type instability occurs.

The proposed numerical procedure has been demonstrated to be fast, stable and accurate, presenting results in excellent agreement with the exact solutions.

Thanks to these benefits, the GDQ method could be efficiently applied to solve linear and nonlinear damped stability problems for nonuniform cantilever beams [38]. Moreover, the present approach could be extended to situations in which coupling between the various forms of motion such as bending, shear and torsion takes place.

## Acknowledgements

This research was supported by the Italian Ministry for University and Scientific, Technological Research MIUR (40% and 60%). The research topic is one of the subjects of the Centre of Study and Research for the Identification of Materials and Structures (CIMEST)—"M. Capurso" of the University of Bologna, Italy.

## References


[1] I. Elishakoff, Controversy associated with the so-called "follower forces": critical overview, *Applied Mechanics Reviews* 58 (2005) 117–142.

[2] M. Beck, Die knicklast des enseiting eingespannten tangential gedruckten stabes, *Zeitschrift fuer Angewandte Mathematik und Physik* 3 (1952) 225–228 (in German).

[3] V.V. Bolotin, *Nonconservative Problems in the Theory of Elastic Stability*, Fitmatgiz Publisher, Moscow, 1961 (in Russian) (English translation, Pergamon Press, New York, 1964).

[4] S.P. Timoshenko, J.M. Gere, *Theory of Elastic Stability*, McGraw-Hill, Auckland, 1963.

[5] S. Nemat-Nasser, *On the Elastic Stability under Nonconservative Forces*, University of Waterloo Press, Waterloo, Ontario, Canada, 1973.

[6] H. Leipholz, *Stability of Elastic Systems*, Sijthoff & Noordhoff, Alphen aan den Rijn, 1980.

[7] D.J. McGill, Column instability under weight and follower loads, *Journal of the Engineering Mechanics Division* 97 (3) (1971) 629–635.

[8] C. Sundasarajan, On the stability and eigencurves of an elastic system subjected to conservative and nonconservative forces, *Zeitschrift fuer Angewandte Mathematik und Physik* 54 (1974) 434–436.

[9] M.A. Langthjem, Y. Sugiyama, Dynamic stability of columns subjected to follower loads: a survey, *Journal of Sound and Vibration* 238 (5) (2000) 809–851.

[10] C. Shu, *Differential Quadrature and its Application in Engineering*, Springer, Berlin, 2000.

[11] E. Viola, F. Tornabene, Vibration analysis of damaged circular arches with varying cross-section, *Structural Integrity and Durability (SID-SDHM)* 1 (2) (2005) 155–169.

[12] E. Viola, F. Tornabene, Vibration analysis of conical shell structures using GDQ method, *Far East Journal of Applied Mathematics* 25 (1) (2006) 23–39.

[13] E. Viola, M. Dilena, F. Tornabene, Analytical and numerical results for vibration analysis of multi-stepped and multi-damaged circular arches, *Journal of Sound and Vibration* 299 (1–2) (2007) 143–163.

[14] F. Tornabene, E. Viola, Vibration analysis of spherical structural elements using the GDQ method, *Computers and Mathematics with Applications* 53 (2007) 1538–1560.

[15] A.N. Sherbourne, M.D. Pandy, Differential quadrature method in the buckling analysis of beams and composite plates, *Computers and Structures* 40 (1991) 903–913.

[16] R.H. Gutierrez, E. Romanelli, P.A.A. Laura, Vibrations and elastic stability of thin circular plates, *Journal of Sound and Vibration* 195 (3) (1996) 391–399.

[17] P. Mirfakhraei, D. Redekop, Buckling of circular cylindrical shells by the differential quadrature method, *International Journal of Pressure Vessels and Piping* 75 (1998) 347–353.

[18] M.A. De Rosa, N.M. Auciello, Two approaches to the dynamic analysis of foundation beams subjected to subtangential forces, *Computers and Structures* 82 (6) (2004) 519–524.

[19] B.N. Rao, G.V. Rao, Applicability of the static criterion for the stability of a cantilever column under a tip-concentrated subtangential follower force, *Journal of Sound and Vibration* 120 (1) (1987) 197–200.

[20] H. Leipholz, Uber die befreiung der Ansatzfunktionen des Ritzschen und galerkinschen verfahrens von den Randbedingungen, *Archive of Applied Mechanics (Ingenieur Archiv)* 36 (1967) 215–261 (in German).

[21] F. Kikuchi, A finite element method for non-self-adjoint problems, *International Journal for Numerical Methods in Engineering* 6 (1973) 39–54.

[22] G.V. Rao, B.N. Rao, Galerkin finite element solution for the stability of cantilever columns subjected to tangential loads, *AIAA Journal* 13 (5) (1975) 690–691.

[23] Z. Elfelsoufi, L. Azrar, Integral equation formulation and analysis of the dynamic stability of damped beams subjected to subtangential follower forces, *Journal of Sound and Vibration* 296 (4–5) (2006) 690–713.

[24] I. Elishakoff, B. Couch, Nonuniform Leipholz's column on elastic foundation—instability study by symbolic algebra, *Solid Mechanics Archives* 12 (1) (1987) 53–63.

[25] B.J. Ryu, Y. Sugiyama, K.B. Yim, G.S. Lee, Dynamic stability of an elastically restrained column subjected to triangularly distributed subtangential forces, *Computers and Structures* 76 (5) (2000) 611–619.

[26] E. Viola, A. Marzani, Crack effect on dynamic stability of beams under conservative and non-conservative forces, *Engineering Fracture Mechanics* 71 (2004) 699–718.

[27] A. Marzani, E. Viola, Effect of boundary conditions on the stability of beams under conservative and non-conservative forces, *Structural Engineering and Mechanics* 16 (2003) 195–217.

[28] H. Leipholz, Die knicklast des enseiting eingespannten stabes mit gleichmassig verteilter, tangentialer langsbelastung, *Archive of Applied Mechanics (Ingenieur Archiv)* 36 (1962) 215–261 [Zeitschrift fuer Angewandte Mathematik und Physik 13 (1962) 581–589 (in German)].

[29] W. Hauger, Die Knicklasten elastischer Stäbe unter gleichmäβig verteilten und linear veränderlichen, tangentialen Druckkräften, *Archive of Applied Mechanics (Ingenieur Archiv)* 35 (4) (1966) 221–229 (in German).

[30] Column Research Committee of Japan, *Handbook of Structural Stability*, Corona Publishing Co., Tokyo, 1971.

[31] M.A. De Rosa, C. Franciosi, The influence of an intermediate support on the stability behaviour of cantilever beams subjected to follower forces, *Journal of Sound and Vibration* 137 (1) (1990) 107–115.

[32] W. Glabisz, Stability of non-prismatic rods subjected to non-conservative loads, *Computers and Structures* 46 (1993) 479–486.

[33] J.T. Katsikadelis, G.C. Tsiatas, Optimum design of structures subjected to follower forces, *International Journal of Mechanical Sciences* 49 (11) (2007) 1204–1212.
[34] H. Leipholz, K. Bhalla, On the solution of the stability problems of elastic rods subjected to triangularly distributed tangential follower forces, *Archive of Applied Mechanics (Ingenieur Archiv)* 46 (1977) 115–124.
[35] Y. Sugiyama, K.A. Mladenov, Vibration and stability of elastic columns subjected to triangularly distributed sub-tangential forces, *Journal of Sound and Vibration* 88 (4) (1983) 447–457.
[36] B. Shvartsman, April 2006, private communication.
[37] E. Viola, I. Bartoli, A. Marzani, Boundary conditions effect on the dynamic instability of orthotropic plates, *Scientific Israel—Technological Advantages* 5 (1) (2003) 66–83.
[38] B. Shvartsman, Large deflections of a cantilever beam subjected to a follower force, *Journal of Sound and Vibration* (available online 4 May 2007).